Chin. Geogra. Sci. 2020 Vol. 30 No. 4 pp. 588–599
https://doi.org/10.1007/s11769-020-1136-x

Springer Science Press
www.springerlink.com/content/1002-0063

Spatial Patterns of LULC and Driving Forces in the Transnational Area of Tumen River: A Comparative Analysis of the Sub-regions of China, the DPRK, and Russia

NAN Ying[1], WANG Bingbing[1], ZHANG Da[1], LIU Zhifeng[2, 3], QI Dekang[1], ZHOU Haohao[1]

(1. *College of Geography and Ocean Sciences*, *Yanbian University*, *Yanji Jilin*, 133002, *China*; 2. *Center for Human-Environment System Sustainability* (*CHESS*), *State Key Laboratory of Earth Surface Processes and Resource Ecology* (*ESPRE*), *Beijing Normal University*, *Beijing* 100875, *China*; 3. *School of Natural Resources*, *Faculty of Geographical Science*, *Beijing Normal University*, *Beijing* 100875, *China*)

Abstract: Understanding the spatial patterns of land-use and land-cover (LULC) and their driving forces in transnational areas is important for the sustainable development of these regions. However, the spatial patterns of LULC and their driving forces across multiple scales are poorly understood in transnational areas. In this study, we analyzed the spatial patterns of LULC and driving forces in the transnational area of Tumen River (TATR) in 2016 across two scales: the entire region and the sub-regions of China, the Democratic People's Republic of Korea (DPRK), and Russia. Results showed that the LULC was dominated by broadleaf forest and dry farmland in the TATR in 2016, which accounted for 66.86% and 13.60% of the entire region, respectively. Meanwhile, the LULC in the three sub-regions exhibited noticeable differences. In the Chinese and the DPRK's sub-regions, the area of broadleaf forest was greater than those for the other LULC types, while the Russian sub-region was dominated by broadleaf forest and grassland. The spatial patterns of LULC were mainly influenced by topography, climate, soil properties, and human activities. In addition, the driving forces of the spatial patterns of LULC in the TATR had an obvious scaling effect. Therefore, we suggest that effective policies and regulations with cooperation among China, the DPRK, and Russia are needed to plan the spatial patterns of LULC and improve the sustainable development of the TATR.

Keywords: land-use and land-cover (LULC); spatial pattern; driving force; transnational area of Tumen River

Citation: NAN Ying, WANG Bingbing, ZHANG Da, LIU Zhifeng, QI Dekang, ZHOU Haohao, 2020. Spatial Patterns of LULC and Driving Forces in the Transnational Area of Tumen River: A Comparative Analysis of the Sub-regions of China, the DPRK, and Russia. *Chinese Geographical Science*, 30(4): 588–599. https://doi.org/10.1007/s11769-020-1136-x

1 Introduction

Transnational areas are regions where two or more countries exist along national boundary lines (Grant and Quinn, 2007). The spatial pattern of land-use and land-cover (LULC) refers to the composition and configuration of various LULC types in the region, reflecting the characteristics of regional LULC under different natural conditions and human activities (Zhang et al., 2008; Pelorosso et al., 2009; Verburg et al., 2011; Hansen and Loveland, 2012; Mao et al., 2018). In transnational areas, the spatial patterns of LULC and their driving forces show a significant difference between countries due to different government policies, socioeconomic conditions and regulations. These differences have placed significant pressure on the sustainable development of entire transnational areas. It is

Received date: 2019-12-22; accepted date: 2020-04-15
Foundation item: Under the auspices of National Natural Science Foundation of China (No. 41771094, 41871185, 41801184)
Corresponding author: ZHANG Da. E-mail: zhangda@ybu.edu.cn

therefore important to quantify and understand the spatial patterns of LULC and their driving forces in transnational areas, an area of investigation which has become highly significant in landscape ecology and sustainability science (Kashaigili and Majaliwa, 2010; Wu et al., 2014; Akhtar et al., 2017).

The transnational area of Tumen River (TATR) is located in the northeastern area of China, covering Jilin Province of China, northeastern areas of the Democratic People's Republic of Korea (DPRK), and southeastern areas of Russia. This region comprises the major area of the 'Major Function Oriented Zoning of China' launched by the Ministry of Environmental Protection and the Chinese Academy of Sciences in 2011, as well as an important part of the 'China-Russia- DPRK-Mongolia' economic zone under 'The Belt and Road Initiative' national strategy launched by the Chinese government (Fang, 2017; Yang et al., 2019). Forest area in this region, an important vegetation cover which provides an important role in maintaining several important ecosystem services, such as biodiversity, water retention, and carbon sequestration, accounts for about 70% of the entire region (Tao et al., 2017; Wang et al., 2020). This region, therefore, is important for the sustainable development of China, the DPRK, and Russia, as well as across northeast Asia (Zhu et al., 2012; Wang et al., 2020). It is of great theoretical and practical significance to quantify and analyze the spatial patterns of LULC and their driving forces in this region.

Recent studies have examined the spatial patterns of LULC and their driving forces in transnational areas. For example, Kashaigili and Majaliwa (2010) assessed the spatial patterns of LULC in the Malaga River Basin, located in the transnational area between Tanzania and Burundi. Wu et al. (2017) analyzed the spatial patterns of LULC and their driving forces in the Cauchy Basin in 2010 (i.e., a transnational region between China and Nepal). However, the existing studies have almost focused on quantifying the spatial patterns of LULC and analyzing their driving forces on a single scale (i.e., the entire region). In the transnational areas, there are significant differences in national government policies, socioeconomic development, and driving forces of LULC among different countries. It is necessary to conduct research on the spatial patterns of LULC and their driving forces on multiple scales, i.e., the entire region and the sub-regions of different countries. This kind of research can provide suggestions for different countries to formulate relevant policies to improve the sustainable development of the transnational areas.

In this study, our objective was to quantify the spatial patterns of LULC and their driving forces across multiple scales in the TATR. This was undertaken by initially obtaining LULC data for 2016 using remote sensing data. Landscape metrics were then used to quantify the spatial patterns of LULC across the entire region and in the sub-regions of China, the DPRK, and Russia. Finally, logistic regression analysis was used to quantify the driving forces of the spatial patterns of LULC across multiple scales.

2 Materials and Methods

2.1 Study area

The TATR, covering an area of 24 000 km^2, is situated between 128°E–133°E and 40°N–44°N (Wang et al., 2020) (Fig. 1). The northern and western areas are located in China and cover an area of 10 100 km^2 (42.09% of the total area), including Yanji, Longjing, Tumen, and Hunchun. Yanji is large city with population exceeding 300 thousand, Longjing, Tumen, and Hunchun are medium cities with population between 100 thousand and 300 thousand (Li et al., 2018; Yang et al., 2019). The southwestern area is located in the DPRK and covers 6800 km^2 (28.33% of the total area), mainly including one large city with population exceeding 300 thousand (i.e., Chongjin) and seven small cities with population below 100 thousand (i.e., Wencheng, Saibie, Ende, Xianfeng, Luojin, Puryong, and Hoeryong) (Li et al., 2018; Yang et al., 2019). The eastern area is located in Russia and covers 7100 km^2 (29.58% of the total area), including one large city with population exceeding 300 thousand (i.e., Vladivostok) and three small cities with population below 100 thousand (i.e., Khasanskiy, Artem, and Nadezhdinskiy) (Li et al., 2018; Yang et al., 2019). Elevation of the TATR is higher in the northeastern area and lower in the southeastern area. The region has a medium temperate monsoon climate. Average annual precipitation is 700–800 mm, and annual average temperature is 2℃–6℃ (Guo et al., 2015).

2.2 Data

Data used in this study included remote sensing data, geographic information system (GIS) ancillary data,

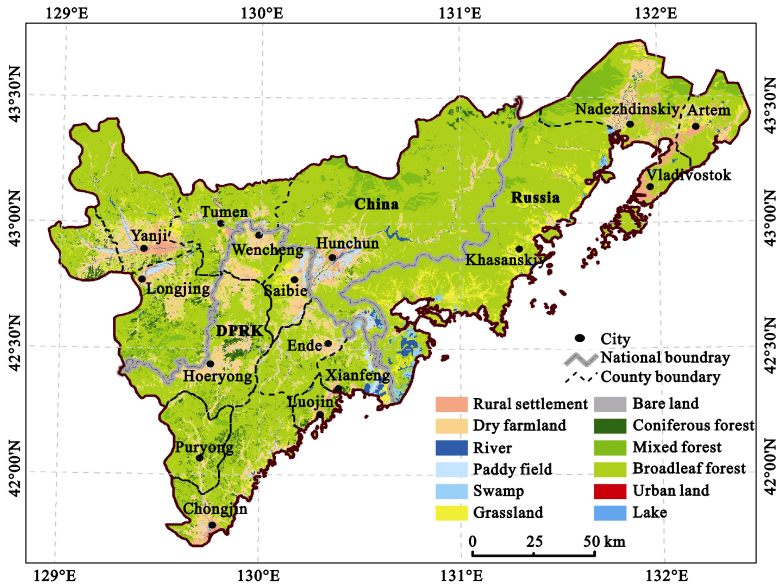

Fig. 1 Location of the transnational area of Tumen River (TATR). LULC data was produced through visual interpretation using Landsat-8 imagery

meteorological data, population density data, nighttime light data, and soil data. The remote sensing data obtained in July and August in 2016 could cover the three sub-regions of China, the DPRK, and Russia with less cloud cover and high radiation resolution. Meanwhile, the year 2016 was the starting year of the 13th Five-Year Plan for Economic and Social Development of the People Republic of China. For these two reasons, LULC for 2016 was selected to analyzing the spatial patterns of LULC and their driving forces in the TATR, which could provide a solid basis for the further analysis of land-use and land-cover change (LUCC) in the next five years. Remote sensing data included Landsat-8 imagery from 2016 (Orbital numbers 114/30, 114/31, 115/30, and 115/31) were obtained from the Geospatial Data Cloud of the Computer Network Information Center of Chinese Academy of Sciences (http://www.gsc-loud.cn). After obtaining these images, we finished geometric correction and radiation correction for these remote sensing data. Then, we extracted these remote sensing data based on the administrative boundaries of TATR. The GIS ancillary data, including administrative boundaries, were obtained from the Chinese National Geographic Information Center (http://ngcc.sbsm.gov.cn) and the Global Administrative Boundaries Dataset (http://www.gadm.org/). Meteorological data, including temperature and precipitation data, were obtained from the global weather station (https://gis.ncdc.noaa.gov). The meteorological data were then converted to raster data by using Kriging interpolation method. Population density data were derived from the History Database of the Global Environment (HYDE) data (http://themasites.pbl.nl/tridion/en/themasites/hyde/). Nighttime light data were acquired from the National Oceanic and Atmospheric Administration (https://www.ncdc.noaa.gov). Soil data were downloaded from the world soil database (http://www.fao.org/soil-survery). All the data were georegistered to the Universal Transverse Mercator Projection coordinate system and resampled to a spatial resolution of 30 m.

2.3 Methods

2.3.1 Extracting LULC information

Methods used to extract LULC information from remote sensing images mainly include supervised classification, unsupervised classification, and visual interpretation (Zhou et al., 2008; Tuia et al., 2009). As visual interpretation can produce LULC data with a higher level of accuracy and reliability compared with supervised classification and unsupervised classification (Tuia et al., 2011; Du et al., 2012), we therefore used visual interpretation to interpret remote sensing images to produce LULC data. Firstly, according to national standards and Nan et al. (2012), we established the classification system of LULC in the TATR. The LULC types included urban land, rural settlement, dry farmland, paddy field, river, lake, swamp, grassland, bare land, coniferous forest, mixed forest, and broadleaf forest. We then performed a visual interpretation based on the interpretation criteria to obtain the LULC information in the TATR for 2016.

After obtained the LULC classifications, we evaluated their accuracy based on high-resolution remotely sensed data from Google Earth in 2016 (Tao et al., 2017). This was undertaken by initially randomly selecting 60 sampling points for each LULC type (720 random points in total) using a stratified random sampling method. The 720 random sampling points were then imported into Google Earth to obtain real LULC information. Finally, the accuracy of the LULC data was evaluated by comparing the classification result of each random point with the real LULC information. The accuracy assessment revealed an overall accuracy of 88.25%, and a Kappa coefficient of 0.87, indicating that the LULC classification result can accurately reflect real LULC information in this region.

2.3.2 Quantifying spatial patterns of LULC

Landscape metrics were used to quantify the spatial patterns of LULC across the entire region and in the three sub-regions in the TATR in 2016 (Zhu et al., 2012; 2014; Wu, 2013; Ma et al., 2014; Tao et al., 2017). The landscape metrics were: patch density (PD), edge density (ED), landscape shape index (LSI), contagion index (CONTAG), mean patch size (MPS), mean patch fractal dimension index (FRAC_MN), and Shannon's diversity index (SHDI) (Table 1). For these landscape metrics, when the values for PD, LSI, CONTAG, FRAC_MN, and SHDI were larger, the fragmentation of the spatial pattern of LULC was larger. Meanwhile, when the values for ED and MPS were smaller, the configuration of the spatial pattern of LULC was simple, and the fragmentation of the spatial pattern of LULC was larger. Fragstats 4.2 software was used to calculate the seven landscape metrics across the TATR and in the sub-regions of China, the DPRK, and Russia.

2.3.3 Analyzing the driving forces of spatial patterns of LULC

A logistic regression analysis was used to analyze the driving forces of the spatial patterns of LULC in the TATR in 2016. In this analysis, $X_n = (x_1, x_2, ..., x_n)$ is a set of independent variables (i.e., driving forces). Y_i is a dependent variable, this being a binary variable used to indicate if the given LULC type i is a certain LULC type or not, where 1 represents a certain LULC type and 0 represents an uncertain LULC type (Wang et al., 2013; Wu et al., 2016). P_i is used to express the probability of the occurrence of LULC type i. In other words, when the pixel values for a LULC type mainly correspond to the pixel values for a specific driving force, it can be said that the spatial pattern of this LULC type is affected by this driving force. When the P_i values are larger, the LULC type i will more likely occur, and vice versa. P_i can be calculated as:

$$\log(P_i) = \ln\left(\frac{P_i}{1-P_i}\right) = \alpha_0 + \alpha_1 x_1 + \alpha_2 x_2 + \ldots + \alpha_n x_n \quad (1)$$

where x_1, x_2, ..., x_n are the driving forces; and α_0, α_1, ..., α_n are the regression coefficients of the driving forces. The positive regression coefficients mean that the spatial patterns of LULC will be positively influenced by the driving forces, and vice versa. Meanwhile, the absolute values of the regression coefficients are used to indicate the contribution of the driving forces.

Based on previous studies and the geographical characteristics in the TATR, eight natural driving forces and four anthropogenic driving forces were selected as the key driving forces of the spatial patterns of LULC in this study. The natural driving forces included elevation, slope, temperature, precipitation, silt content, sand content, clay content, and distance to the nearest river, meanwhile, the anthropogenic driving forces included population, intensity of nighttime light, distance to the nearest town, and distance to the nearest road (Ye et al., 2001; Zhou et al., 2008; Sun et al., 2015).

Table 1 Landscape metrics used in this study

Landscape metrics	Abbreviation	Description
Patch density	PD	The number of patches per hectare (num/ha), reflecting landscape fragmentation
Edge density	ED	The total length of all edge segments per hectare (m/ha)
Landscape shape index	LSI	A modified perimeter-area ratio that measures the shape complexity of the patch
Contagion index	CONTAG	Used to describe the degree of agglomeration or extended trend of different block types in the landscape
Mean patch size	MPS	The average area of all patches in the landscape (ha)
Mean patch fractal dimension index	FRAC_MN	The value of the fractal dimension is one to two. If value is closer to one, the shape of the patch is simpler, and vice versa
Shannon's diversity index	SHDI	Used to describe the diversity or heterogeneity of landscape types

In order to analyze the driving forces of the spatial patterns of LULC at multiple scales, firstly, random points (totally 27 000 points) in the three sub-regions of China, the DPRK, and Russia were selected using a stratified random sampling method. Then, the LULC information and the values of driving forces of each random point were extracted. Finally, the information of LULC and the values of driving forces were imported into the SPSS software, and the logistic regression model was used to analyze the driving forces of the spatial patterns of LULC in the TATR and the sub-regions of China, the DPRK, and Russia.

3 Results

3.1 LULC in the TATR

Broadleaf forest (16 055.11 km^2) and dry farmland (3265.69 km^2) covered the greatest area of the TATR, respectively (Fig. 2). Grassland was the next largest area (1169.52 km^2), accounting for 4.87% of the total area, whilst lakes and bare land (combined area of 138.33 km^2) accounted for the smallest areas (less than 1.00% of the total area).

Analysis of LULC results for the three sub-regions (China, the DPRK, and Russia) indicated noticeable differences between the LULC types. In China, broadleaf forest (7156.32 km^2; 70.68%) and dry farmland (1241.77 km^2; 12.26%) occupied the greatest area, followed by mixed forest (431.30 km^2; 4.26%) (Fig. 2). Lakes and bare land covered the smallest area. In the DPRK, broadleaf forest (4174.48km^2; 61.08%) and dry farmland (1594.78km^2; 23.34%) were the dominant LULC types. In Russia, broadleaf forest and grassland (totally accounting for 77.43%) accounted for the greatest area of coverage, while coniferous forest and bare land accounted for the smallest area, accounting for only 0.14% of the total area in the sub-region.

3.2 Spatial patterns of LULC

In the TATR, the fragmentation of coniferous forest was the largest, followed by broadleaf forest and grassland, and the fragmentation of urban land and bare land was the smallest. PD and LSI values for coniferous forest were 0.46 and 142.08, respectively, higher than the other LULC types (Fig. 3). Meanwhile, MPS value for coniferous forest was 6.74 ha, lower than the other LULC types except for bare land. PD values for broadleaf forest and grassland were 0.35 and 0.30, respectively, while PD values for urban land and bare land were both lower than 0.01. In addition, ED, MPS, LSI, and FRAC_MN values for bare land were 0.02 m/ha, 4.95 ha, 8.49, and 1.05, respectively.

In the three sub-regions, the fragmentation of LULC was the greatest in China, followed by the DPRK, and then Russia (Fig. 4). By analyzing the values for PD, LSI, and CONTAG, the PD value for LULC was 2.04, and the LSI and CONTAG values were 79.15 and 72.37, respectively, which meant that the configuration of LULC was complex in China. In the sub-region of the DPRK, the LSI and CONTAG values for LULC were 75.70 and 71.04, respectively, meaning the configuration of LULC was simple. In addition, in the sub-region of Russia, the PD, LSI, CONTAG, and SHDI values were 0.66, 50.43, 71.86, and 1.24, respectively.

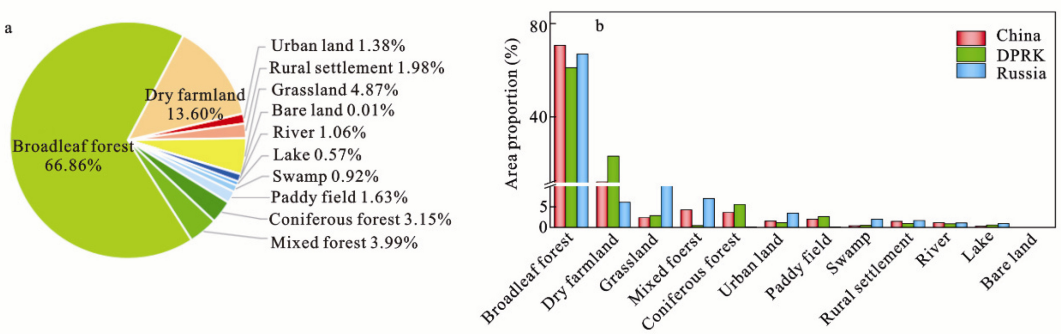

Fig. 2 The proportion of LULC in the TATR (a) and in the sub-regions of China, the Democratic People's Republic of Korea (DPRK), and Russia (b) in 2016. Area proportion represents the proportion of each LULC to the total area in the sub-regions of China, the DPRK, and Russia

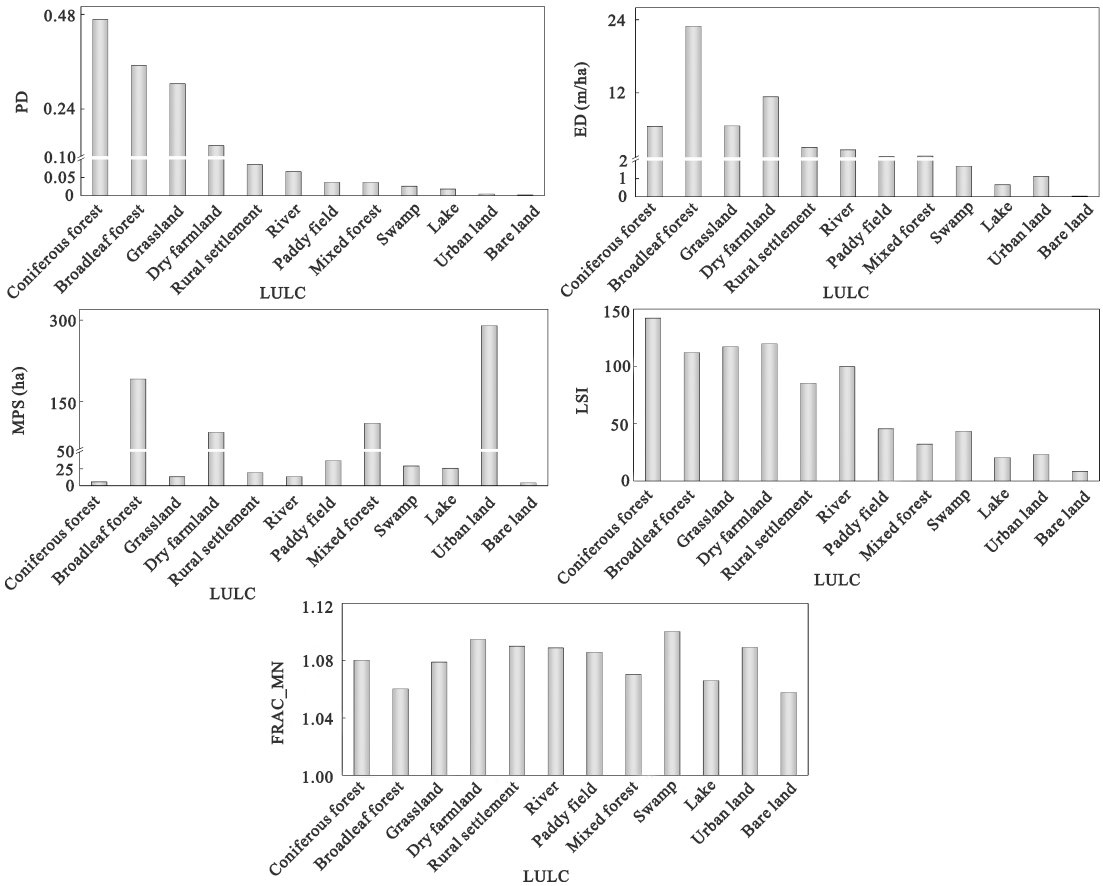

Fig. 3 Landscape metrics of different LULC in the transnational area of Tumen River (TATR). Meanings of abbreviations see Table 1

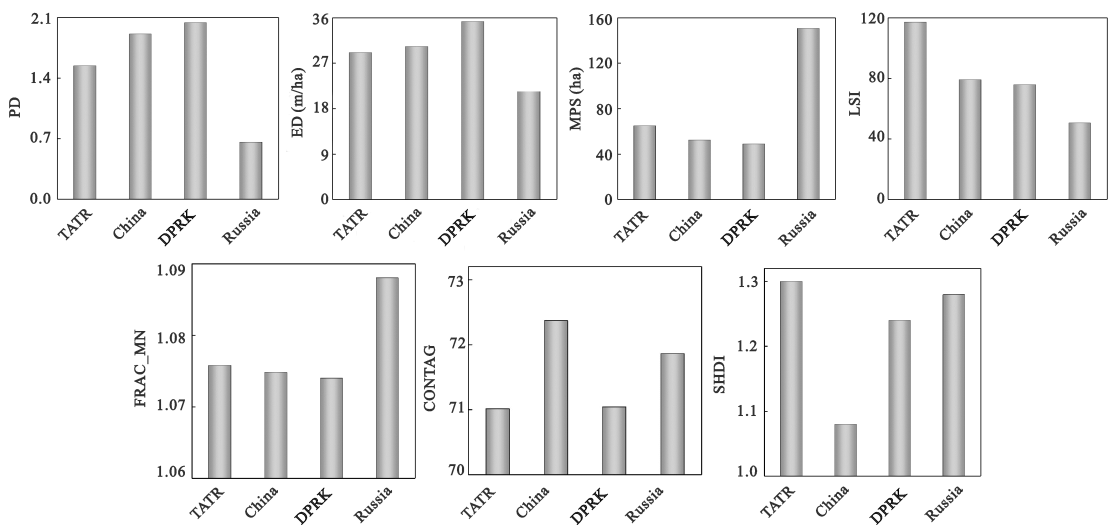

Fig. 4 Landscape metrics of LULC in the entire region and the sub-regions of China, the DPRK, and Russia. Meanings of abbreviations see Table 1

3.3 Driving forces of spatial patterns of LULC in the TATR

For the spatial pattern of broadleaf forest, among the natural driving forces, temperature had the greatest effect (Table 2), with the regression coefficient of 0.56. Meanwhile, the regression coefficients of the other important natural driving forces (i.e., slope, elevation, and precipitation) were 0.51, 0.47, and 0.29, respectively.

Among the anthropogenic driving forces, the most important one affected the spatial pattern of broadleaf forest was intensity of nighttime light, with the regression coefficient of –0.61.

For the spatial pattern of dry farmland which had the second largest area, the major natural driving forces were temperature and elevation, with the regression coefficients of –0.92 and –0.77, respectively (Table 2). Among the anthropogenic driving forces, the most important one was distance to the nearest road, with the regression coefficient of –0.52. Meanwhile, for the spatial pattern of grassland which had the third largest area across the entire TATR, the major natural driving forces were elevation (–0.69) and clay content in soil (0.39). Furthermore, among the anthropogenic driving forces, distance to the nearest road and intensity of nighttime light had a significant influence on the spatial pattern of grassland.

For the spatial pattern of urban land, the anthropogenic driving forces (including population, intensity of nighttime light, and distance to the nearest town) were the main driving forces (Table 2). The increase in population and nighttime light intensity meant the increase in artificial buildings. Therefore, the spatial pattern of urban land had a positive correlation with nighttime light intensity and population, with the regression coefficients of 1.07 and 0.22, respectively. Among the natural driving forces, the most important forces that affected the spatial pattern of urban land were elevation and slope, with the regression coefficients of –1.52 and –0.93, respectively. In the TATR, urban land was usually distributed in the areas with low altitude and low slope. For this reason, the spatial pattern of urban land was negatively correlated with elevation and slope.

3.4 Driving forces of spatial patterns of LULC in the sub-regions

In the three sub-regions of China, the DPRK, and Russia, the driving forces of spatial patterns of LULC showed significant differences. For the LULC type which covered the greatest area of the TATR (i.e., broadleaf forest), in the sub-region of China, the spatial pattern of broadleaf forest had a positive correlation with elevation and slope, with the regression coefficients of 1.12 and 0.76, respectively (Table 3). Meanwhile, among the anthropogenic driving forces, intensity of nighttime light influenced the spatial pattern of broadleaf forest negatively, with the regression coefficient of –3.97. In the sub-region of the DPRK, the spatial pattern of broadleaf forest was positively related with the natural driving forces except for distance to the nearest river, while negatively related with intensity of nighttime light (–2.10) and population (–0.09). In addition, in the sub-region of Russia, the most important force that affected the spatial pattern of broadleaf forest was elevation, with the regression coefficient of 0.51.

Table 2 Regression coefficients of driving forces of spatial patterns of LULC in the TATR

Driving forces	Indices	Broadleaf forest	Mixed forest	Coniferous forest	Grassland	River	Lake	Swamp	Paddy field	Dry farmland	Urban land	Rural settlement
Natural	Elevation	0.47*	0.99*	0.62*	–0.69*	–1.12*	–2.12*	–3.20*	–2.11*	–0.77*	–1.52*	–0.94*
	Slope	0.51*	–	0.20*	–0.28*	–1.05*	–0.77*	–	–2.04*	–0.54*	–0.93*	–0.63*
	Temperature	0.56*	0.20*	–0.77*	–	–	–0.72*	–0.38*	–1.25*	–0.92*	–	0.32*
	Precipitation	0.29*	0.66*	0.50*	–0.30*	0.64*	1.25*	–	–	0.13*	–	–0.81*
	Silt content in soil	–	–	0.24*	–0.14*	–	0.37*	0.34*	0.64*	0.13*	–	–
	Sand content in soil	–	0.17*	–	–	–	–	–0.67*	–0.39*	0.17*	–	–
	Clay content in soil	0.12*	–	–0.38*	0.39*	–	–0.41*	–0.58*	–0.38*	–0.16*	–	–0.20*
	Distance to the nearest river	–	–	–	0.21*	–220.02*	0.45*	–1.90*	–0.71*	–	0.37*	0.22*
Anthropogenic	Population	–0.28*	–0.24*	–0.17*	–	0.71*	–	–	–	0.14*	0.22*	–
	Intensity of nighttime light	–0.61*	–19.61*	–0.91*	–0.23*	–	–	–	–0.25*	–0.42*	1.07*	0.29*
	Distance to the nearest town	0.21*	–0.50*	–0.37*	–	0.41*	0.62*	1.03*	–0.41*	–0.26*	–10.24*	–0.30*
	Distance to the nearest road	0.09*	1.03*	–	–0.27*	–	–	–0.94*	–	–0.52*	–	–1.54*

Notes: * denotes that correlation is significant at 0.05 level. – represents the driving force was excluded from logistic regression analysis

Table 3 Regression coefficients of driving forces of spatial patterns of LULC in the sub-regions of China, the DPRK, and Russia

Driving forces		Broadleaf forest			Mixed forest			Coniferous forest			Grassland			River			Lake		
		C	D	R	C	D	R	C	D	R	C	D	R	C	D	R	C	D	R
Natural	Elevation	1.12*	1.64*	0.51*	1.70*	2.74*	2.42*	–	0.23*	28.08*	–0.32*	–0.50*	–0.31*	–2.16*	–1.25*	–0.95*	–3.27*	–2.78*	–8.56*
	Slope	0.76*	0.55*	0.01*	–	–	–	–	–	–	–0.49*	–	–	–1.10*	–0.53*	–0.49*	–1.54*	–3.18*	–2.32*
	Temperature	0.32*	–	0.05*	–	–	0.49*	–1.36*	–0.54*	–12.34*	–	1.22*	–	–	–	–	–0.96*	–	–0.80*
	Precipitation	0.28*	0.63*	0.05*	1.06*	–	–	1.03*	0.70*	–	–0.67*	–0.99*		–	–0.34*	–	–	–	–
	Silt content in soil	–0.17*	–	–	–0.48*	–	–	–0.51*	–1.57*	–	–	–	–0.06*	–	–	–	–0.69*	–	–
	Sand content in soil	0.15*	0.73*	–	0.30*	–	–	–	–	–	–	–	–0.02*	–	–	–	–	–	–
	Clay content in soil	–	0.55*	0.07*	–	–	–0.60*	–0.43*	–1.38*	–	–	–	0.10*	–	–	–	–	–	–
	Distance to the nearest river	–	–0.19*	–	0.58*	–	–	–	–	–	–	0.55*	0.06*	–53.01*	–112.06*	–92.16*	–	–	–
Anthropogenic	Population	–	–0.09*	–0.10*	–	–	–44.85*	–	–	–	–	–	–	0.54*	–	–	0.71*	–	–
	Intensity of night-time light	–3.97*	–2.10*	–0.13*	–	–1.35*	–	–	–0.24*	–	–1.19*	–0.26*	–0.21*	–	–	–	–	–1.96*	–
	Distance to the nearest town	0.26*	–	–	–0.50*	–	–1.89*	0.35*	–0.40*	–	–0.24*	–	0.05*	–	–	0.34*	–	–	–
	Distance to the nearest road	0.51*	0.26*	–	–	–	0.51*	–	–	–	–0.47*	–0.48*	–	–	–	–	–	–	–

Driving forces		Swamp			Paddy field			Dry farmland			Urban land			Rural settlement		
		C	D	R	C	D	R	C	D	R	C	D	R	C	D	R
Natural	Elevation	–3.65*	–5.98*	–14.51*	–3.53*	–2.59*	–0.94*	–1.20*	–1.52*	–4.52*	–1.35*	–0.92*	–1.61*	–1.31*	–2.59*	–1.26*
	Slope	–	–	–	–4.36*	–2.27*	0.36*	–0.74*	–0.39*	–1.84*	–2.53*	–0.87*	1.52*	–0.67*	–2.27*	–0.93*
	Temperature	–2.86*	–	–0.53*	–	–0.58*	1.97*	–0.17*	–0.29*	–	–	–	0.91*	–	–0.58*	–
	Precipitation	2.12*	0.86*	–	–	–	–	–0.38*	–0.48*	–0.77*	0.69*	–	–	–0.66*	–	–
	Silt content in soil	2.31*	–	–	1.10*	–1.20*	0.11*	–	–2.73*	–	–	–	–	–	–	–
	Sand content in soil	–	–	–	–	–	–	–	–	–	–	–	–	–	–	–
	Clay content in soil	–	–	–0.89*	–	–	–	–	2.55*	0.43*	–	–	–	–	–	–0.59*
	Distance to the nearest river	–4.79*	–	–1.70*	–1.31*	–0.96*	–2.56*	0.16*	0.25*	–0.68*	–	–	–	–	–	–
Anthropogenic	Population	–	–	–	–	–	–	–	–	–	0.92*	0.54*	1.05*	0.12*	0.22*	0.46*
	Intensity of night-time light	–	–	–	–0.64*	0.29*	–	–0.27*	–	–0.58*	25.10*	0.14*	0.85*	–	0.29*	–
	Distance to the nearest town	3.23*	1.49*	2.57*	–1.14*	–	–	–0.30*	–	–1.72*	–68.12*	–51.23*	–82.15*	–	–	–
	Distance to the nearest road	–	–1.10*	–	–	–	–	–0.52*	–0.26*	–	–0.49*	–	–5.03*	–1.16*	–1.63*	–20.30*

Notes: * denotes that correlation is significant at 0.05 level. – represents the driving force was excluded from logistic regression analysis. C, China; D, DPRK; R, Russia

For the LULC type which covered the second largest area in the TATR (i.e., dry farmland), in the sub-region of China, elevation (–1.20) was the major natural driving force, and distance to the nearest road (–0.52) was the most important anthropogenic driving force (Table 3). In the sub-region of the DPRK, among the natural driving forces, silt content had the greatest effect, with the regression coefficient of –2.73; among the anthropogenic driving forces, the most important force was distance to the nearest road, with the regression coefficient of –0.26. In addition, in the sub-region of Russia, elevation (–4.52) was the most important natural driving force, and distance to the nearest town (–1.72) was the major anthropogenic driving force.

In addition, for the LULC type which was most affected by human activities (i.e., urban land), the anthropogenic driving forces were the major forces in the three sub-regions. Among the anthropogenic driving forces, distance to the nearest town was the most influential driving force in the three sub-regions. The regression coefficients were –68.12, –51.23, and –82.15 in the sub-regions of China, the DPRK, and Russia, respectively, which were significantly higher than the other driving forces (Table 3).

4 Discussion

4.1 Changes of driving forces of spatial patterns of LULC across different scales

According to Wu (2004) and Ma et al. (2018), scaling usually refers to the translation of information across spatial and temporal scales or organizational levels, which frequently involves changing grain size, extent, or both. Recently, several studies have shown that the driving forces of spatial patterns of LULC have an obvious scaling effect on different scales (Huang et al., 2009; Ma et al., 2016). In other words, the influences of driving forces of spatial patterns of LULC will change across different scales. This is of great significance for understanding the drivers of LULC and formulating land management policies. In this study, we found that the driving forces of spatial patterns of LULC changed across different scales in the TATR. Across the entire TATR, the influences of natural driving forces were greater than those of anthropogenic driving forces for all LULC types. For all LULC types, the number of natural driving forces influencing the spatial patterns of LULC exceeded that of anthropogenic driving forces (Table 2). Meanwhile, the regression coefficients of natural driving forces were generally greater than those of anthropogenic driving forces.

On the other hand, we found that the influences of anthropogenic driving forces gradually increased from the entire TATR to the three sub-regions of China, the DPRK, and Russia. For example, for the LULC type which covered the greatest area of the TATR (i.e., broadleaf forest), the absolute values of regression coefficients of anthropometric driving forces increased from 0.09–0.61 for the whole TATR to 0.09–3.97 for the three sub-regions (Table 3). For another LULC type which covered a large area in the TATR (i.e., dry farmland), the absolute values of regression coefficients of anthropometric driving forces increased from 0.14–0.52 at the regional scale to 0.26–1.72 at the sub-region scale. In addition, for the LULC type which was most affected by human activities (i.e., urban land), the influences of anthropometric driving forces of the three sub-regions were significantly higher than those of the whole region, with the absolute values of regression coefficients increasing from 0.22–10.24 to 0.14–82.15. This finding showed that the spatial patterns of LULC were mainly influenced by natural driving forces in the whole TATR, while in the three sub-regions of China, the DPRK, and Russia, the influences of anthropometric driving forces significantly enhanced.

4.2 Implications for land resource management and sustainable development in the TATR

In the TATR, land resource management has become an important issue. The sub-region of China has experienced a rapid urban expansion in recent years (Yang et al., 2019). Meanwhile, in the DPRK, food security problem due to arable land loss is always serious. In addition, deforestation and reclamation of cropland are commonly used to address the severe food security problem in the DPRK. This kind of deforestation and cropland reclamation have already caused serious soil erosion and natural habitat loss for several decades. Therefore, how to effectively manage land resources and promote regional sustainable development have become important issues in this transnational area.

At present, China, the DPRK, and Russia have issued a series of policies to manage land resources in the TATR. In China, ‘Land Management Law of the Peo-

ple's Republic of China' and 'The Overall Plan for Land Utilization of Yanbian Korean Autonomous Prefecture from 1997 to 2010' were issued in 1998 and 2005, respectively. In 1977, the DPRK's government issued the 'Land Law of Democratic People's Republic of Korea', which pointed out that 'land development and urban expansion must not occupy cropland, as far as possible to protect high-quality cropland'. Meanwhile, the DPRK's government issued 'Environmental Conservation Management Law' in 1998 and 'Environmental Protection Law' in 1999. In Russia, 'Natural Resources Protection Law' and 'Agricultural Land Circulation Law of the Russian Federation' have been launched in 1993 and 2003, respectively (Prishchepov et al., 2013). These policies have produced positive effects in managing land resources and promoting sustainable development of the TATR. However, there are still several serious problems to be solved, such as natural habitat loss, deforestation, and cropland loss (Yang et al., 2019). Therefore, based on the major findings of this study, we suggest that: firstly, forest was positively correlated with elevation in the whole TATR and the three sub-regions of China, the DPRK, and Russia. Meanwhile, both dry farmland and paddy field were negatively correlated with elevation. Therefore, forest at high elevations should be regarded as ecological protection red line to reduce land reclamation in the high elevation area, which was usually happened in the DPRK during the past several decades. Secondly, in this study, we found that urban land, dry farmland, and paddy field were all negatively correlated with elevation, that is urban land and cropland were distributed at low altitudes in the TATR and the three sub-regions of China, the DRPK, and Russia. Therefore, we should pay attention to protect important cropland distributed around cities at low altitudes. Finally, China, the DPRK, and Russia should strengthen their cooperation and conduct effective measures for the sustainable utilization of land resources and the regional sustainable development in the TATR.

4.3 Future perspectives

This study has certain limitations. First, we only analyzed the LULC of the TATR in 2016 and the driving forces of spatial patterns of LULC, the temporal-spatial dynamics of LULC over a long period was not quantified. Second, we analyzed the driving forces of spatial patterns of LULC using statistical methods, rather than analysis from the mechanism. However, these limitations will not fundamentally affect the results above. We analyzed the spatial patterns of LULC and driving forces in the TATR in 2016 on multiple scales. The outcome of this study will play an important role in understanding the driving forces of LULC and promoting the sustainable development in this transnational area.

In the future, more remote sensing data will be used to analyze the temporal-spatial dynamics of LULC in this region, more auxiliary data will be used to analyze the driving forces of spatial patterns of LULC (He et al., 2014). We will also attempt to analyze the spatial patterns of LULC and changes from the angle of mechanism, rather than only use statistical method (Ma et al., 2016). In addition, we will attempt to quantify the LUCC and forecast its impacts on the sustainable management of land resources in the TATR in the near future (Zhang et al., 2017; 2019).

5 Conclusions

In this study, we analyzed the spatial patterns of LULC in the TATR (transnational area of Tumen River) on two scales, i.e., the entire region and the three sub-regions of China, the DPRK (Democratic People's Republic of Korea), and Russia using remote sensing images. Then, logistic regression analysis was used to analyze the driving forces of spatial patterns of LULC on different scales. We found that broadleaf forest and dry farmland were the main LULC types in the TATR in 2016, accounting for 66.86% and 13.60% of the total land area, respectively. Meanwhile, these two LULC types occupied the greatest area in the sub-region of China, as well as the sub-region of the DPRK. In addition, broadleaf forest and grassland were the two dominant LULC types in the sub-region of Russia.

In the TATR, elevation and slope were the major natural driving forces, while distance to the nearest town was the major anthropogenic driving force. In the three sub-regions, the spatial patterns of LULC were mainly affected by elevation, slope, nighttime light intensity, and distance to the nearest town. In addition, the driving forces of spatial patterns of LULC changed across different scales. Across the entire TATR, the influences of natural driving forces were greater than those of anthropogenic driving forces for all LULC types. Meanwhile, the influences of anthropogenic driving forces

gradually increased from the entire TATR to the three sub-regions of China, the DPRK, and Russia. This finding showed that the spatial patterns of LULC were mainly influenced by natural driving forces in the entire TATR, while in the three sub-regions, the influences of anthropometric driving forces enhanced. Based on our findings, we suggest that it is of great significance for understanding the driving forces of spatial patterns of LULC at multiple scales in the transnational area to formulate land management policies. For the TATR, China, the DPRK, and Russia should strengthen their cooperation and conduct effective measures for the sustainable utilization of land resources and the regional sustainable development.

References

Akhtar F, Awan U K, Tischbein B, 2017. A phenology based geo-informatics approach to map land use and land cover (2003–2013) by spatial segregation of large heterogenic river basins. *Applied Geography*, 88: 48–61. doi: org/10.1016/j.apgeog.2017.09.003

Du P J, Xia J S, Zhang W et al., 2012. Multiple classifier system for remote sensing image classification: a review. *Sensors*, 12(4): 4764–4792. doi: 10.3390/s120404764

Fang Chuanglin, 2017. The strategy and pattern of international economic cooperation in Tumen River area of China under the 'the Belt and Road'. *Northeast Asia Economic Research*, 1(1): 5–14. (in Chinese)

Grant J A, Quinn M S, 2007. Factors influencing transboundary wildlife management in the North American 'Crown of the Continent'. *Journal of Environmental Planning and Management*, 50(6): 765–782. doi: 10.1080/09640560701609323

Guo X Y, Zhang H Y, Wang Y Q et al., 2015. Mapping and assessing typhoon-induced forest disturbance in Changbai Mountain National Nature Reserve using time series Landsat imagery. *Journal of Mountain Science*, 12(2): 404–416. doi: 10.1007/s11629-014-3206-y

Hansen M C, Loveland T R, 2012. A review of large area monitoring of land cover change using Landsat data. *Remote Sensing of Environment*, 122(1): 66–74. doi: 10.1016/j.rse.2011.08.024

He C Y, Liu Z F, Tian J et al., 2014. Urban expansion dynamics and natural habitat loss in China: a multiscale landscape perspective. *Global Change Biology*, 20(9): 2886–2902. doi: 10.1111/gcb.12553

Huang Qingxu, He Chunyang, Shi Peijun et al., 2009. Understanding multi-scale urban expansion driving forces: in the case study of Beijing. *Economic Geography*, 29(5): 714–721. (in Chinese)

Kashaigili J J, Majaliwa A M, 2010. Integrated assessment of land use and cover changes in the Malagarasi river catchment in Tanzania. *Physics and Chemistry of the Earth*, *Parts A/B/C*, 35(13–14): 730–741. doi: 10.1016/j.pce.2010.07.030

Li B, Liu Z F, Nan Y et al., 2018. Comparative analysis of urban heat island intensities in Chinese, Russian, and DPRK regions across the transnational urban agglomeration of the Tumen River in Northeast Asia. *Sustainability*, 10(8): 2637. doi: 10.3390/su10082637

Ma Q, He C Y, Wu J G, 2016. Behind the rapid expansion of urban impervious surfaces in China: major influencing factors revealed by a hierarchical multiscale analysis. *Land Use Policy*, 59: 434–445. doi: 10.1016/j.landusepol.2016.09.012

Ma Q, He C Y, Wu J G et al., 2014. Quantifying spatiotemporal patterns of urban impervious surfaces in China: an improved assessment using nighttime light data. *Landscape and Urban Planning*, 130: 36–49. doi: 10.1016/j.landurbplan.2014.06.009

Ma Q, Wu J G, He C Y et al., 2018. Spatial scaling of urban impervious surfaces across evolving landscapes: from cities to urban regions, *Landscape and Urban Planning*, 175: 50–61. doi: 10.1016/j.landurbplan.2018.03.010

Mao D H, Wang Z M, Wu J G et al., 2018. China's wetlands loss to urban expansion. *Land Degradation & Development*, 29: 2644–2657.

Nan Ying, Ji Zhe, Dong Yehui et al., 2012. Study of land use/cover dynamic change in Tumen River across national border region during the last 30 years. *Journal of Natural Science of Hunan Normal University*, 35(1): 82–89. (in Chinese)

Pelorosso R, Leone A, Boccia L, 2009. Land cover and land use change in the Italian central Apennines: a comparison of assessment methods. *Applied Geography*, 29(1): 35–48. doi: 10.1016/j.apgeog.2008.07.003

Prishchepov A V, Müller D, Dubinin M et al., 2013. Determinants of agricultural land abandonment in post-Soviet European Russia. *Land Use Policy*, 30(1): 873–884. doi: 10.1016/j.landusepol.2012.06.011

Sun Q L, Feng X F, Ge Y et al., 2015. Topographical effects of climate data and their impacts on the estimation of net primary productivity in complex terrain: a case study in Wuling Mountainous area, China. *Ecological Informatics*, 27(27): 44–54. doi: 10.1016/j.ecoinf.2015.02.003

Tao H, Nan Y, Liu Z F et al., 2017. Spatiotemporal patterns of forest in the transnational area of Changbai Mountain from 1977 to 2015: a comparative analysis of the Chinese and DPRK sub-regions. *Sustainability*, 9(6): 1054. doi: 10.3390/su9061054

Tuia D, Ratle F, Pacifici F et al., 2009. Active learning methods for remote sensing image classification. *IEEE Transactions on Geoscience and Remote Sensing*, 47(7): 2218–2232. doi: 10.1109/TGRS.2008.2010404

Tuia D, Volpi M, Copa L et al., 2011. A survey of active learning algorithms for supervised remote sensing image classification. *IEEE Journal of Selected Topics in Signal Processing*, 5(3): 606–617. doi: 10.1109/JSTSP.2011.2139193

Verburg P H, Neumann K, Nol L, 2011. Challenges in using land

use and land cover data for global change studies. *Global Change Biology*, 17(2): 974–989. doi: 10.1111/j.1365-2486.2010.023.07.x

Wang J W, Zhang D, Nan Y et al., 2020. Spatial patterns of net primary productivity and its driving forces: a multi-scale analysis in the transnational area of the Tumen River. *Frontiers of Earth Science*, 14(1): 124–139. doi: 10.1007/s11707-019-0759-7

Wang N H, Brown D G, An L et al., 2013. Comparative performance of logistic regression and survival analysis for detecting spatial predictors of land-use change. *International Journal of Geographical Information Science*, 27(10): 1960–1982. doi: 10.1080/13658816.2013.779377

Wu J G, 2004. Effects of changing scale on landscape pattern analysis: scaling relations. *Landscape Ecology*, 19(2): 125–138. doi: 10.1023/B:LAND.0000021711.40074.ae

Wu J G, 2013. Landscape sustainability science: ecosystem services and human well-being in changing landscapes. *Landscape Ecology*, 28(6): 999–1023. doi: 10.1007/s10980-013-9894-9

Wu Jianguo, Guo Xiaochuan, Yang Jie et al., 2014. What is sustainability science? *Chinese Journal of Applied Ecology*, 25(1): 1–11. (in Chinese)

Wu L, Deng F, Xie Z et al., 2016. Spatial analysis of severe fever with thrombocytopenia syndrome virus in China using a geographically weighted logistic regression model. *International Journal of Environmental Research and Public Health*, 13(11): 1125. doi: 10.3390/ijerph13111125

Wu Xue, Gao Jungang, Zhang Yili et al., 2017. Land cover status in the Koshi River Basin, Central Himalayas. *Journal of Resources and Ecology*, 8(1): 10–19. doi: 10.5814/j.issn.1674-764x.2017.01.003

Yang Y M, Zhang D, Nan Y et al., 2019. Modeling urban expansion in the transnational area of Changbai Mountain: a scenario analysis based on the zoned Land Use Scenario Dynamics-urban model. *Sustainable Cities and Society*, 50: 101622. doi:10.1016/j.scs.2019.101622

Ye Baoying, Huang Fang, Zhang Shuwen et al., 2001. The driving forces of land use/cover change in the upstream area of the Nenjiang River. *Chinese Geographical Science*, 11(4): 377–377. doi: 10.1007/s11769-001-0054-9

Zhang D, Huang Q X, He C Y et al., 2017. Impacts of urban expansion on ecosystem services in the Beijing-Tianjin-Hebei urban agglomeration, China: a scenario analysis based on the Shared Socioeconomic Pathways. *Resources*, *Conservation and Recycling*, 125: 115–130. doi: 10.1016/j.resconrec.2017.06.003

Zhang D, Huang Q X, He C Y et al., 2019. Planning urban landscape to maintain key ecosystem services in a rapidly urbanizing area: a scenario analysis in the Beijing-Tianjin-Hebei urban agglomeration, China. *Ecological Indicators*, 96: 559–571. doi: 10.1016/j.ecolind.2018.09.030

Zhang X P, Zhang L, Zhao J et al., 2008. Responses of streamflow to changes in climate and land use/cover in the Loess Plateau, China. *Water Resources Research*, 44(7): W00A07. doi: 10.1029/2007WR006711

Zhou W Q, Troy A, Grove M, 2008. Object-based land cover classification and change analysis in the Baltimore metropolitan area using multitemporal high resolution remote sensing data. *Sensors*, 8(3): 1613–1636. doi: 10.3390/s8031613

Zhu Weihong, Guo Yanli, Sun Peng et al., 2012. Wetland ecosystem health assessment of the Tumen River downstream. *Acta Ecologica Sinica*, 32(21): 6609–6618. (in Chinese)

Zhu Weihong, Miao Chengyu, Zheng Xiaojun et al., 2014. Study on ecological safety evaluation and warning of wetlands in Tumen River watershed based on 3S technology. *Acta Ecologica Sinica*, 34(6): 1379–1390. (in Chinese)